Integrated aerodynamic/electrochemical microsystem for collection and detection of nanogram-level airborne bioaccessible metals

Yi-Bo Zhao [a,b], Jiukai Tang [a,b], Tianyu Cen [c,d], Guangyu Qiu [a,b], Weidong He [a,b,e], Fuze Jiang [a,b], Ranxue Yu [a,b,f], Christian Ludwig [c,d], Jing Wang [a,b,*]

[a] *Institute of Environmental Engineering, ETH Zürich, 8093 Zürich, Switzerland*
[b] *Advanced Analytical Technologies, Empa, Ueberlandstrasse 129, 8600 Dübendorf, Switzerland*
[c] *Environmental Engineering Institute (IIE, GR-LUD), School of Architecture, Civil and Environmental Engineering (ENAC), École Polytechnique Fédérale de Lausanne (EPFL), 1015 Lausanne, Switzerland*
[d] *Bioenergy and Catalysis Laboratory (LBK-CPM), Energy and Environment Research Division (ENE), Paul Scherrer Institut (PSI), 5232 Villigen, Switzerland*
[e] *Filter Test Center, School of Resources and Civil Engineering, Northeastern University, NO. 3-11, Wenhua Road, Heping District, Shenyang, Liaoning 110819, China*
[f] *Key Laboratory of Textile Science & Technology, Ministry of Education, College of Textiles, Donghua University, No. 2999 North Renmin Road, Songjiang, Shanghai 201620, China*

ARTICLE INFO

ABSTRACT

The soluble fraction of aerosol particulate matter containing trace metals has the potential to engender toxicity and exacerbate the adverse health effects of particulate matter. In this study, an inertial-impaction-based fluidic chip integrated with electrochemical detection was developed to achieve high collection efficiency and measurements of the bioaccessible metal fraction at the nanogram level. The average collection efficiency for ultrafine and fine particles larger than 50 nm, obtained at a flow rate of 2.5 L/min, was above 70%. The detection ranges of aerosol soluble copper depended on the collection duration and airflow rate. At a working flow rate of 3.1 L/min and collection efficiency of 70%, the microsystem was capable of detecting Cu concentrations above 53 ng/m^3, 32 ng/m^3 and 8 ng/m^3 with 3 h, 5 h and 20 h collection periods, respectively, which were in the range of reported atmospheric concentrations. The detection ratio of real-world samples (i.e. PM$_{10}$-like aerosol) was 100 ± 14%, indicating excellent aerodynamic collection and reliable electrochemical detection. The collection and sensing performance of the microsystem demonstrates a new step towards an online, mobile, low-cost, and miniaturized routine monitoring system for bioaccessible metals and possibly other soluble components in the aerosols.

1. Introduction

Particulate matter, containing trace metals emitted from anthropogenic and natural sources, is of an environmental concern which moreover affects human health [1] and geochemical cycles [2]. It has been widely recognized that heavy metals engender toxicity and exacerbate the negative health effects of atmospheric particulate matter, and they require comprehensive monitoring and understanding [3]. The chemical speciation of atmospheric heavy metals is crucial to the bioavailability and toxicities of the aerosol particles [4–6]. In particular, the soluble fraction (bioaccessible) of aerosol metals are more easily released into the body fluid of the human physiological system compared to non-soluble metals [5]. Soluble metals in particulate matter

such as copper (Cu) are able to produce reactive oxygen species, resulting in oxidative stress and negative health effects [7]. Traditional networks of stationary monitoring are scattered geographically and monitor the air quality at a low spatiotemporal resolution [8]. More comprehensive monitoring and understanding of the aerosol metals at concentrations as low as nanogram level per cubic meter are required. However, this entails some difficult tradeoffs between complicated coupling and miniaturized system, for example between spatiotemporal resolution and cost, that affects air quality control and exposure evaluation greatly [8]. The real-time and spatially resolved routine monitoring of nanogram-level aerosol bioaccessible metals requires the development and combination of advanced aerosol sampling and detection techniques, which offers an opportunity for an

---

interdisciplinary study involving aerodynamics, electrochemistry and engineering design to develop and miniaturize the sensing platform.

Highly efficient aerosol sampling is the crucial step prior to the detection of chemical components of particles, and aerosol samplers such as the impactor [9,10], aerosol-into-liquid collector [11,12] and electrostatic air sampler [13,14] have been developed. In some cases, additional components such as saturation-condensation and particle-to-droplet growth parts are essential to improve the collection efficiencies of fine and ultrafine particulate matter [10]. To achieve a miniaturized system for particle collection, some lab-on-a-chip designs based on centrifugal and drag force have been used to collect airborne particles [15,16], and bacterial aerosols [17–20]. A microimpinger has been developed as a compact way to the aerosol-into-liquid collector and liquid-based sampler [21]. Nonetheless, the relatively low sampling volume rate of air (< 100 mL/min) is less likely to provide sufficient samples within several hours for further detection, compared to high volume samplers.

The available detection techniques of trace metals include electrochemical [22,23] and optical methods [24–27]. Electrochemistry is one of the methods that enables the rapid detection of trace soluble metals with good selectivity and sensitivity [28], and miniaturized sensing system can be realized without significant loss of sensitivity [29]. Electrochemical detection methods such as voltammetry are a viable alternative to ICP-MS measurements [30] as evidenced by their applications to aqueous samples such as drinking water [31], river samples [32] and polluted water [33]. Electrochemical techniques enable the detection of metals such as Cu, Cd, Pb, Fe, Ni [34], and also allow the miniaturization of detection system integrated with microfluidics [35]. The microfluidics techniques allow a significantly reduced amount of samples, faster diffusion of chemicals and so on [36]. There are several studies focusing on the development of microfluidics platform integrated with electrochemical electrodes for heavy-metal detection in water samples [37–39]. Nonetheless, the integration of microfluidics and electrochemical detection techniques with aerosol sampling techniques has not been sufficiently developed [40]. For instance, microfluidic techniques are mainly applied as aerosol sampling units to couple with detection instruments such as mass spectrometry. The available studies tend to combine microfluidic electrochemical sensors and aerosol collectors in series to measure aerosol oxidative activity [41], sulfate and nitrate [42].

Because of the relatively low concentration of aerosol metals especially soluble species, proper aerosol collection and detection may impose important limits on the instrument that might result in a bulky benchtop setup. Indeed, conventional instruments such as ICP-MS require complex equipment, laborious operation and professional personnel [34]. Some newly developed and portable techniques such as X-ray fluorescence (XRF), is not able to distinguish soluble fraction from total concentration [27]. There are limited pioneering studies focusing on the offline or online detection of aerosol metal samples using electrochemical detection techniques to achieve more rapid, low-cost and portable aerosol collection and determinations (Table 1) [9,11,34, 43–47]. Available studies mainly focus on the passive collection of atmospheric deposits, the coupling to an instrument and the determination of aerosol metals, which may lead to the requirement of a bulky setup or a long time period for collection and measurement. Greater strides should be made towards online, low-cost and mobile sampling and detection systems by better integrating aerosol active sampling and electrochemical detection. To our best knowledge, the integration of electrochemical detection of metal and aerosol sampling has not been realized on the same miniaturized fluidic platform.

In this study, for the first time, the aerosol collection and electrochemical detection of nanogram-level aerosol soluble metals were achieved in an integrated micro-platform. The collection efficiency and sensing performance were investigated and optimized. Cu is one of the relatively abundant elements in the atmosphere, which can cause adverse health effect by inducing oxidative stress [7], and the concentration of aerosol Cu is at the nanogram level per cubic meter, with a soluble fraction of 20–60% [48]. In the proof-of-concept experiment, lab-generated Cu aerosol and PM_{10}-like aerosol were chosen as the target. The concentration of aerosol Cu and PM_{10}-like samples determined by the integrated microsystem was analyzed and further validated by ICP-MS measurements.

2. Experimental section

2.1. Chemicals and apparatus

Sulfuric acid (95–98%), acetic acid ($>$ 98%), Zinc(II) nitrate hexahydrate (98%), lead(II) nitrate (99.999%), cadmium(II) nitrate tetrahydrate (99.997%), potassium hydroxide ($\geq$ 85%), Isopropyl alcohol (IPA) and malachite green solution were obtained from Sigma. Copper (II) nitrate hemi(pentahydrate) (98%) and calcium nitrate tetrahydrate (99%) were purchased from Alfa Aesar. Iron (III) sulfate pentahydrate (97%) was obtained from Acros organics. Di-Ethyl-Hexyl-Sebacate

Table 1
List of studies of aerosol metal sampling and electrochemical detection.

Target metals	Sampling method	Sampling time	Detection method	Time resolution	Detection limit	Operation mode	Refs.
Cd(II) Pb(II) Cu (II) Fe(II) Ni (II)	Ultrasonic personal aerosol sampler	–	Janus electrochemical paper-based devices	–	0.5 µg/L for Cd, Pb, Fe 1 µg/L for Cu and Ni	Offline	[34]
Co(II) Ni(II)	Filters	–	Nafion/Bi carbon stencil-printed electrodes	–	1 µg/L for Co and 5 µg/L for Ni	Offline	[43]
Zn(II) Cd(II) Pb (II)	Ultrasonic personal aerosol samplers and 2.5 µm cut-point cyclones	–	AgNP/Bi/Nafion-modified electrodes	–	5 µg/L for Zn, 0.5 µg/L for Cd and 0.1 µg/L for Pb	Offline	[44]
Cd(II) Pb(II)	Digital DAH-80 high-volume air sampler	24 h	Sputtered-bismuth screen-printed electrodes	–	11.82 µg/L for Cd and 6.07 µg/L for Pb	Offline	[45]
Cu(II)	Total atmospheric deposition polyethylene collectors	7 days	Screen-printed gold electrodes	–	3.7 µg/L	Offline	[46]
Pb(II)	High-volume sampler	24 h	Unmodified screen-printed carbon electrode	–	0.023 µg/L	Offline	[84]
Pb(II) Cu(II)	Atmospheric sampler	24 h	Screen-printed gold electrodes	$>$ 24 h	7.3 µg/L for Cu and 15.1 µg/L for Pb	Online	[47]
Cu(II)	Two virtual impactors combined with a modified liquid impinger (BioSampler)	2–4 h	Copper ion selective electrode	2–4 h	10 µg/L	Online	[9]
Cu(II)	An aerosol-into-liquid collector (saturator tank, condensation tubes and high flow rate impactor)	2–4 h	Copper ion selective electrode	2–4 h	10 µg/L	Online	[11]

(DEHS) was obtained from TOPAS. The electrochemical electrode containing three electrodes with a thickness of 150 nm on a glass substrate (ED-SE1-AuPt) were purchased from MicruX Technologies. Electrochemical measurements were conducted using Bio-Logic 300 electrochemical workstation (Bio-Logic, France).

2.2. Design and modeling of the microchannel collector

To design a microchannel collector with a proper dimension, simulation of air flow, pressure drop and particle collection was performed using the fluid flow and particle tracing modules in COMSOL Multiphysics 5.4. We assumed that particles stick to the wall once particles contact the wall, and drag force affects particle movement. Particle tracing for fluid flow module was used for simulating the particle movement. The collection efficiency was calculated by releasing 5000 particles with a particle density of 2.2 g/cm^3 at a defined velocity. A channel ($\sim$ 220 μL) with a relatively large cross section area (1.6 mm × 1.6 mm) was used to accommodate air flow speed up to 60 m/s and avoid immediate blockage, and the rectangular cross section was chosen for integrating the electrochemical electrode on one side. The ratio of the radius of curvature to the channel diameter was set to 2 [15]. Based on the critical Reynolds number $Re = 2300$), the laminar flow or turbulent flow model was chosen. In this study, the air flow that went through the microchannel inlet (ø1 mm) was assumed turbulent flow, and the k-omega SST turbulence model was used to calculate the flow near the wall and in the free stream (please see details about mesh independence and boundary conditions in the Supporting information).

2.3. Fabrication of aerosol collection and detection microsystem

The microchannel mold was designed using Auto CAD 2019 and subsequently the microchannel mold was printed using a 3D printer. It was sputtered with 50 nm gold to facilitate efficient peeling-off of Polydimethylsiloxane (PDMS) from the mold. PDMS monomer (Sylgard 184, Dow Corning, Midland, USA) was mixed with the curing agent in the volume ratio of 10:1, and degassed in a vacuum desiccator. Then the PDMS gel was cast onto the mold and the cured PDMS was peeled off after being heated at 70 °C for four hours. Three PDMS layers and the electrode with the glass substrate were bonded after 1 min plasma treatment (Fig. 1). The microsystem with a dimension of 35 * 25 * 6 mm consisted of a microchannel (cross section 1.6 * 1.6 mm) and electrochemical electrode. In this way, electrochemical measurement could be performed immediately after aerosol collection in the microchannel without sample transferring and loss, which provides a choice to achieve in situ measurements of atmospheric metals.

Previous studies indicate the residual uncrosslinked oligomers leach from the bulk polymer into the aqueous medium [49,50], and acids introduced into PDMS microchannel are able to modify the topography of the microchannel wall [51]. Therefore, the microchannel wall surface needs to be treated after peeling-off to alleviate the influence on the sensing performance. The microsystem was heated in oven at 70 °C for 5 days to ensure the full polymerization of PDMS chains [52,53]. 0.05 M sulfuric acid and 0.1 M acetate buffer were introduced into microsystem for 6 h in sequence to increases the chemical resistance to sulfuric acid and acetate buffer, and then IPA was added to clean the microchannel for 24 h. 20 μM Cu(NO$_3$)$_2$ solution was used to generate Cu aerosol (i.e. Cu(NO$_3$)$_2$ particles) for 12 h to form temporary coating on microchannel wall. Subsequently, 30 min ultrasonication in a bath with 0.1 M acetate buffer was applied, which eliminates the possible chemical reaction between Cu ion and microchannel surface. Prior to each sensing test, it should be heated at 70 °C for 1 h to stabilize the microchannel wall. The changes of surface chemical groups due to the cleaning of the microchannel were measured using Fourier transform infrared (FTIR) spectroscopy (Cary 600 series, Agilent, USA).

2.4. Aerosol collection and electrochemical measurements

To characterize the particle collection efficiency, NaCl particles (from 1 wt% solution) and DEHS liquid droplet (from 0.5 wt% solution in IPA) were generated using a homemade atomizer at a pressure of
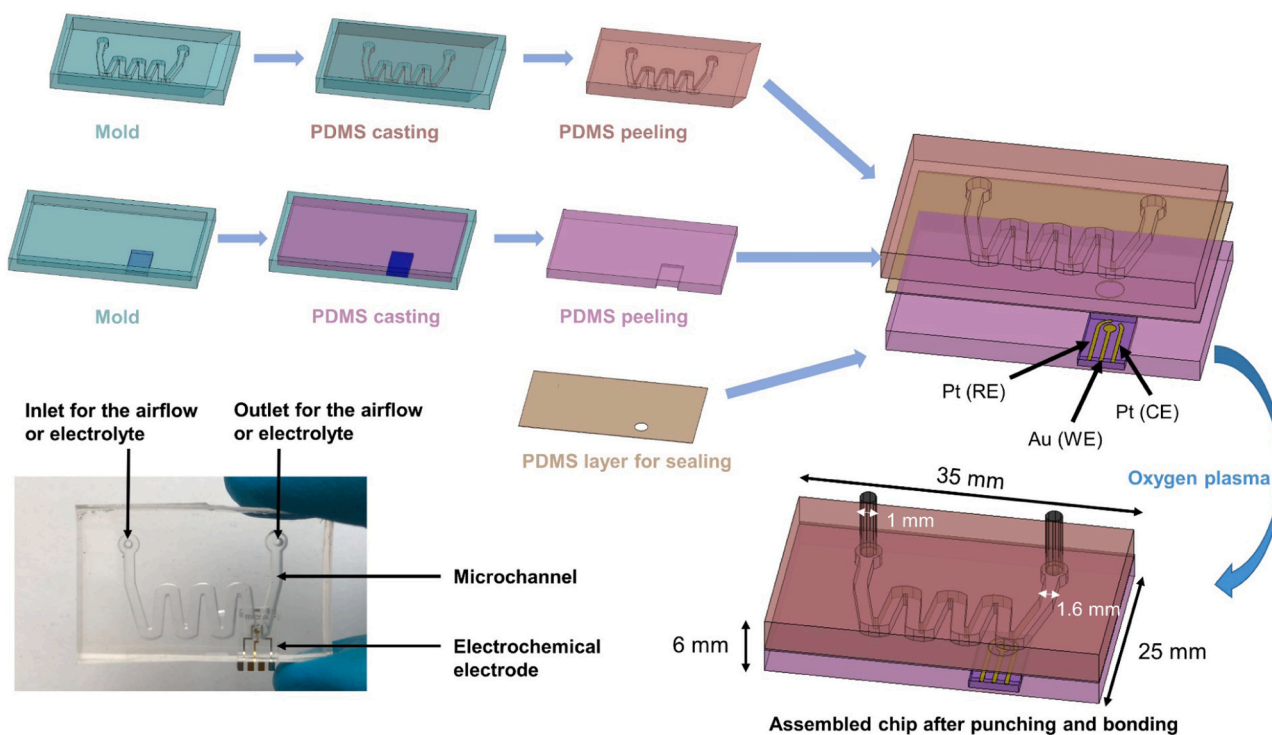

Fig. 1. The fabrication schematic and photo of the integrated aerodynamic/electrochemical microsystem for aerosol collection and electrochemical detection (RE: reference electrode; WE: working electrode; CE: counter electrode).

2.8 bar. The particle size distribution of the generated Cu aerosol in terms of electrical mobility diameter was measured by a Scanning mobility particle sizer (SMPS) consisting of a Differential Mobility Analyzer (DMA, model 3080, TSI, USA) and Condensation Particle Counter (CPC, model 3775, TSI, USA). A DMA (DMA, model 3082, TSI, USA) was used to generate monodisperse aerosols, and the particle numbers before (C_{up}) and after (C_{down}) the microsystem were determined by CPC simultaneously (Fig. S1). The collection efficiency (η) was calculated based on the following equation:

$$\eta = \frac{C_{up} - C_{down}}{C_{up}} \times 100\%$$

Besides Ag/AgCl, platinum and carbon have been widely used as the pseudo reference electrode [54]. In this study, the working electrode (ø1 mm), counter electrode and reference electrode of the electrochemical electrode were gold, platinum and platinum, respectively. Pt electrode was used as the reference electrode for two reasons. Firstly, ultrasonic treatment was applied prior to electrochemical measurements, so the reference electrode should be stable and robust. Secondly, a smaller electrode was needed to be integrated into the microsystem compared to common screen-printed electrodes. The small electrode with a Pt reference electrode used in the work was commercially available and could be easily obtained. Previous studies suggested that 0.1 M acetate buffer in the pH range of 4–5 was used as the supporting electrolyte [55]. Based on this, 0.1 M acetate buffer (pH 4.45) was chosen as the working electrolyte, and KOH was used to adjust the pH of acetic acid solution. Here 2 μL 0.1 M acetate buffer without or with Cu (NO$_3$)$_2$ was used as the sample to evaluate the electrochemical performance of the bare electrode without integrating the microchannel. The open circuit potential (OCP) was measured vs. conventional Ag/AgCl (SI Analytics, 3 M KCl) in 0.1 M acetic acid (pH 4.45). The temporal stability test indicated that the Pt electrode potential was relatively stable for at least 30 min at a value of 0.589 ± 0.016 V vs. Ag/AgCl (Fig. S2). The electrochemical electrode was pre-cleaned in 2 μL 0.05 M H$_2$SO$_4$ for 12 cycles between − 0.9 and 1.3 V at a scan rate of 100 mV/s prior to each use to avoid the reduction of the active area of the electrode occupied by impurities. It is noted that sulfuric acid should not be introduced into the entire microchannel to avoid the formation of a thin organosulfate particle layer [56]. Instead, the sulfuric acid only covered the electrode area for performing the electrochemical cleaning. Before collecting aerosol particles, the microchannel saturated with 0.1 M acetate buffer was cleaned in an ultrasonic bath for 2 min to remove any reaction product between PDMS and acetic acid. Cyclic voltammetry (CV) was conducted in 0.1 M acetate buffer (pH 4.45) with/without Cu ions at a scan rate of 100 mV/s to determine the potential window of the electrode operation and the position of the Cu oxidation peak. Square Wave Anodic Stripping Voltammetry (SWASV) was performed for quantifying metal content in the liquid phase with the presence of dissolved oxygen [57]. The deposition conditions and stripping parameters including pulse width, step potential and SW amplitude, were optimized prior to the determination of aerosol samples. The conditioning potential was set to 0.2 V for 2 min, to preclean any impurities on the electrode surface before Cu deposition. The calibration was performed using three randomly chosen electrodes to determine the working range with minimal variation of Cu current peak height.

5 μM Cu(NO$_3$)$_2$ solution was used to generate Cu aerosol and the electrochemical detection was performed after particle collection and ultrasonic treatment. Ultrasonication for 2 min was used to accelerate the dissolution of water-soluble elements [58,59] and mass transport to possibly reach the distribution equilibrium of Cu ion concentration in the microchannel. The electrolyte samples containing the dissolved airborne Cu after the electrochemical detection were eluted for further ICP-MS validation. To trace and visualize the collection and dissolution of copper ions in the microchannel, Malachite green solution (1 wt% in MiliQ water) was used to generate the aerosol, which was water-soluble and particle-free.

For the evaluation using real-world samples, 0.15 g PM10-like (trace elements) ERM® Certified Reference Material (European Reference Materials, ERM-CZ120) collected in Warsaw, Poland, containing 462 mg Cu in 1 kg sample [60], was suspended in 50 mL Milli-Q water and shaken on a vortex shaker (uniTEXER, LLG Labware) at 1000 rpm for 5 min, followed by sonication for 30 min [61]. This reaerosolization method is able to generate the representative real-world ambient particulate matter, which agrees well with the original ambient aerosol physically and chemically [61]. After the electrochemical detection, the testing solution in the microsystem was filtered using 0.2 μm PTFE syringe filter (Whatman, Maidstone, UK) to separate the insoluble part from the liquid samples, which was not detectable by the electrode in the microsystem. In this study, only the soluble part was measured and verified with ICP-MS measurement.

2.5. Collection and sensing strategies of aerosol trace metals

In general, the procedure for collection and sensing was collecting aerosols with a pump connected to the outlet of the microsystem, and 2 min ultrasonic treatment was applied to homogenize metal ions, prior to electrochemical measurements. The aerosol was aspirated into the microchannel, and the particles were captured on the wall of the microchannel including the area around the inlet, which was the air/solid interface in the particle collection process. After particle collection on the microchannel wall, the liquid (electrolyte)/solid interface for the particle dissolution process was also formed when the leaching agent was introduced. 0.1 M acetate buffer was the leaching agent and electrochemical electrolyte for extracting and detecting bioaccessible trace metals, to maintain metal ions in a free form instead of complex form, with a higher diffusion coefficient during the deposition step [62]. It should be noted that different leaching agents could result in different bioaccessible fractions, and acetate buffer was used for the mild extraction [6,48]. The relatively low volume of the microchannel (~ 220 μL) offered a chance to appropriately concentrate the nanogram-level water soluble trace metals in the liquid phase. No conventional preprocessing such as acid digestion was needed prior to electrochemical sensing. Ultrasonic treatment was applied to increase the dissolution rate and mass transport of Cu(II) ions to reach an equilibrium of concentration gradient prior to the electrochemical sensing stage, resulting in a liquid suspension. This should give reproducible concentrations at the electrode, translating into repeatable electrochemical signals, which was the detection ratio (concentration measured by the microsystem/average concentration in the sample). The detection electrode was placed in the last turn of the microchannel (Fig. 1) to avoid significant fouling by larger particles collected near the inlet.

3. Results and discussion

3.1. Aerosol collection performances of the microsystem

According to the verification of the experiments and simulations, the collection efficiency of NaCl particles in the size range of 50–550 nm is above 60% and 70% at 2 and 2.5 L/min, respectively (Fig. 2a). The maximal working flow rate in the lab is about 3.1 L/min, so the expected collection efficiency of the microsystem at 3.1 L/min was above 70%. The sampling tests and simulations of DEHS particles also show that the collection efficiency of small particles with a lower density (0.9 g/cm^3) was above 60% (Fig. S3). Specifically, the proposed microsystem collects about 80% of 0.5 μm particles, which is comparable to the typical collection efficiency of the reported lab-on-a-chip designs of above 50% [15,21]. According to the simulation shown in Fig. 2b, the high flow rate of above 40 m/s occurs unevenly in the W-shape microchannel, especially in the area closer to the outlet. The flow velocity near the electrode is about 10 m/s (Fig. 2b). The working flow rate above 2.5 L/min brings about a higher pressure drop than CPC could withstand to measure the
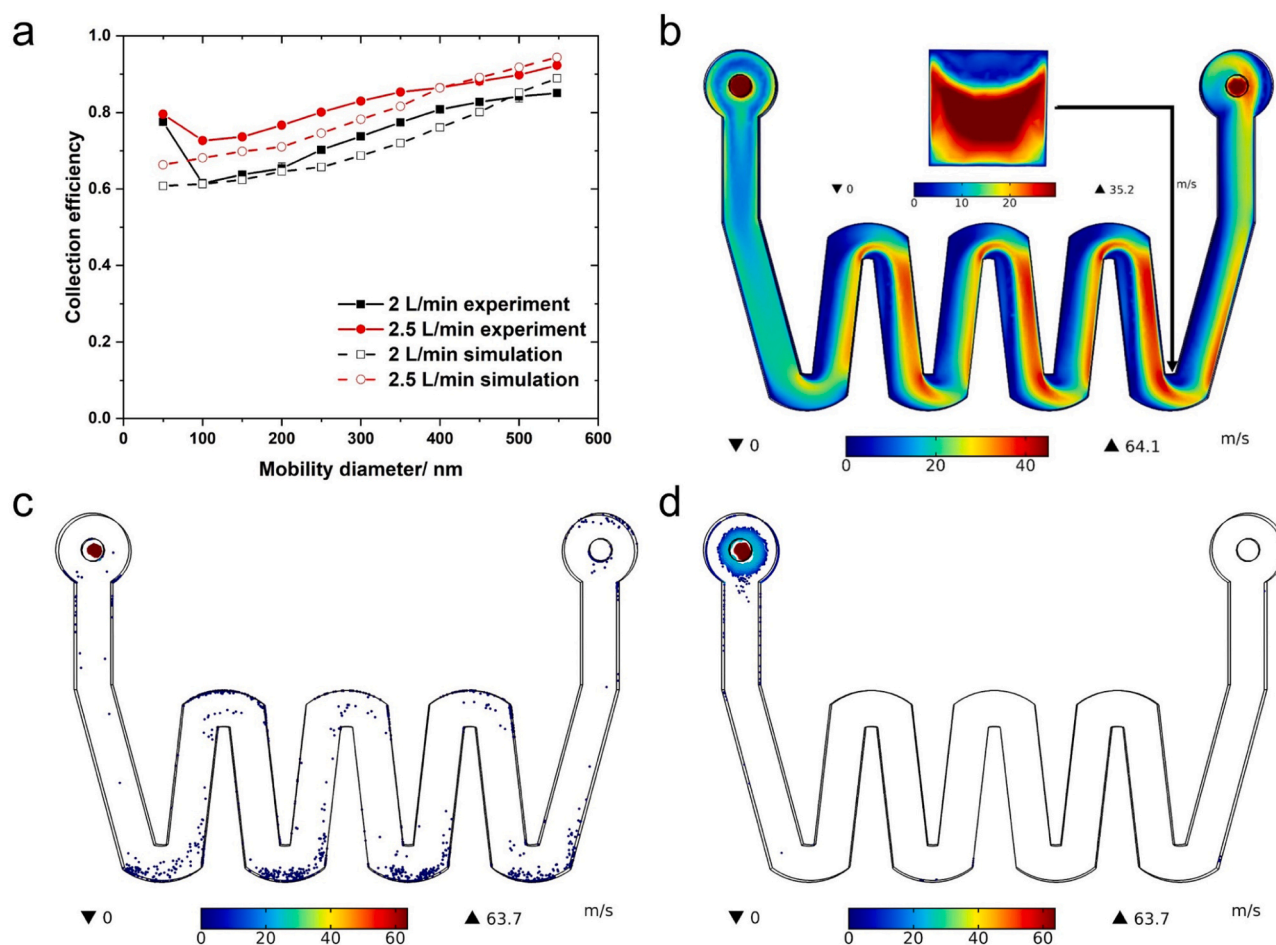
Fig. 2. (a) Calculated and experimental aerosol collection efficiency of NaCl particles in the size range of 50–550 nm (Assuming density: 2.2 g/cm^3) at 2 and 2.5 L/min. (b) Simulated air flow at 3 L/min in the microchannel including the cross section where the electrochemical electrode is. (c) Simulated distribution of collected 50 nm NaCl particles at 3 L/min in the microchannel. (d) Simulated distribution of collected 800 nm NaCl particles at 3 L/min in the microchannel.

downstream particle number. The simulation results of particle transport at 3.0 L/min indicate particles are collected in the microchannel, including the inlet and the microchannel (Fig. 2c and d). Small particles such as 50 nm are collected around the inlet and the microchannel wall over the length of the entire channel, whereas 800 nm particles at a high speed are impacted mainly on the inlet (Fig. 2c and d). In general, the microchannel is used to collect particles with a diameter of less than 1 μm (Fig. 2d), thereby protecting the electrode from contamination by large particles such as black carbon [63] and mineral dust [64]. Compared to the larger inlet (ø 1.6 mm) applied for the microchannel, the smaller inlet with a diameter of 1 mm leads to turbulent flow and increases collection efficiency, lowering the particle size of 100% capture (Fig. S4). The threshold particle diameter with 100% collection efficiency at 1.5, 2.25 and 3 L/min are decreased from 1.75 μm, 1.5 μm and 750 nm to 1.25 μm, 1 μm and 500 nm, respectively (Fig. S4a and b). Therefore, in this work, 1 mm was chosen as the inlet diameter to increase the collection efficiency. At 3 L/min, the PDMS microchannel is able to withstand a pressure drop up to 13.6 kPa (i.e. 0.13 atm) (Fig. S5).

3.2. Electrochemical characterization of the electrode and optimization of SWASV parameters

As shown in Fig. 3a, the Au working electrode in 0.1 M acetate buffer is able to provide a wide potential window in the range of − 0.8 to 0.6 V. In the Cu-free acetate buffer, the onset of oxygen reduction and hydrogen evolution are at about − 0.3 and − 0.8 V, respectively. The oxidation and reduction peaks of Cu in 10 μM solution are at about − 0.2

and − 0.25 V, respectively (Fig. 3a), whereas three oxidation peaks of Cu appear at − 0.4, − 0.3 and − 0.2 V in 1 mM Cu solution, which are linked to two overpotential deposition and one underpotential deposition of Cu on the gold electrode surface, respectively. The onset of hydrogen evolution varies as shown in Fig. 3a, indicating that a slight potential shift may occur in each measurement due to the Pt pseudo-reference used in the work.

After determining the potential window and positions of the oxidation and reduction peak of Cu, the SWASV parameters are optimized using a bare electrode without microchannel, including deposition potential, deposition time, pulse width, step potential and square wave (SW) amplitude, to stabilize and maximize the signal current peak and to improve the peak sharpness. Considering the effect of hydrogen evolution and oxygen reduction, we need to carefully select the deposition potential. It is noted that a potential shift of stripping current peak occurs when the deposition potential is more negative than − 0.9 V due to the significant hydrogen evolution. The current peak becomes stable with a deposition potential more negative than − 0.5 V, exhibiting a coefficient of variation in the range of 7–44% (Fig. 3b). The relatively stable stripping current peaks also suggest that the potential shift owing to the Pt reference electrode has a limited effect on the Cu deposition with the deposition potential in the range of − 0.5 to 0.9 V. Since the deposition potential of Pb and Cd is close to that of Cu [65], a more negative potential applied in the deposition process may lead to the deposition of Pb and Cd. Therefore, − 0.6 V is chosen as the deposition potential to alleviate the interferences from Pb and Cd. The deposition time affects the limit of detection and repeatability of the
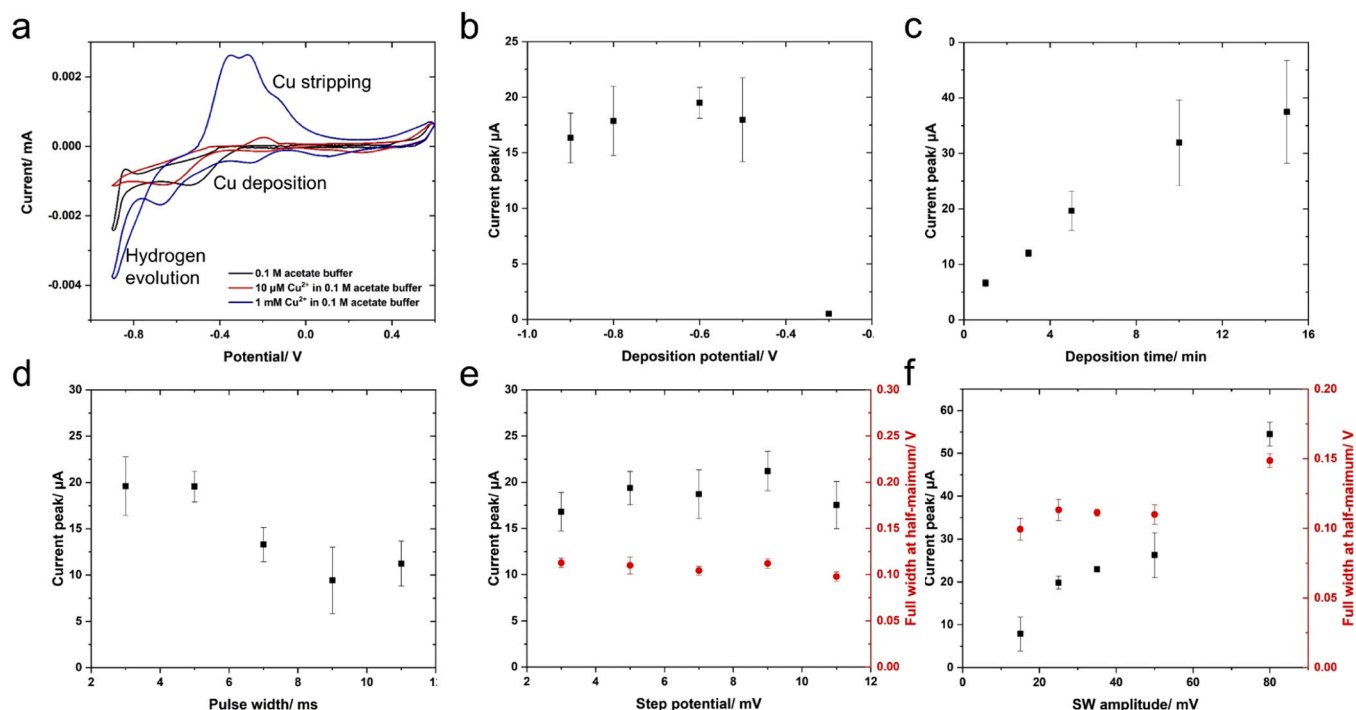
Fig. 3. Cyclic voltammetry of the bare electrode without microchannel (a) and optimization of SWASV parameters: (b) deposition potential; (c) deposition time; (d) SW amplitude; (e) step potential; (f) pulse width in 0.1 M acetate buffer containing 10 μM Cu. The red and black data points indicated full-width at half-maximum and current peak, respectively.

electrochemical electrode [66]. In this study, the deposition times in the 1–15 min range are explored (Fig. 3c). The overpotential deposition occurs when the deposition time is above 5 min likely due to the continuous deposition of Cu on the Cu layer (overpotential deposition) rather than on the Au layer (underpotential deposition), which causes the relatively large variation of current peaks up to 25%.

The results indicate that the current peak decreases by up to 50% with different pulse widths (Fig. 3d). Both sharpness and height of the current peaks are important for the measurement of the target metal in the aerosol samples with complex components, therefore, we use the full width at half-maximum (FWHM) as a second factor to select for optimal values of step potential and SW amplitude [66]. The step potential has a minor influence on FWHM and the current peak is relatively higher with the step potential between 5 and 9 mV (Fig. 3e). In contrast, the increasing SW amplitude causes a significant 35% increase in FWHM, which means that the resolution of the current peak deteriorates and the quantitative analysis of specific metals suffers due to possible current peaks overlap [66] (Fig. 3f). In summary, − 0.6 V, 3 min, 5 ms, 5 mV,

and 35 mV were the optimal values selected for deposition potential, deposition time, pulse width, step potential, and SW amplitude, respectively.

3.3. Sensing performance of the trace metal ions in the liquid phase

The calibration curve shown in Fig. 4a indicates that the limit of detection of the bare electrode is 300 nM in the standard Cu solution, which is 10 times higher than in some previous studies [67]. It suggests that the mass transport of target metals is less efficient, likely owing to not stirring the solution. Here the limit of detection is defined as the threefold background value. The current peak as a function of Cu(II) concentration increases linearly in the range of 300–3000 nM and 3–10 μM, respectively (Fig. 4a). However, the variation of the current peak in the range of 3–10 μM among different electrodes is much larger than that in the range of 300–3000 nM, which indicates an inconsistent performance of different electrodes in the sensing of high concentrations of Cu. According to the SWV current peak of Cu, the Cu current peak is at
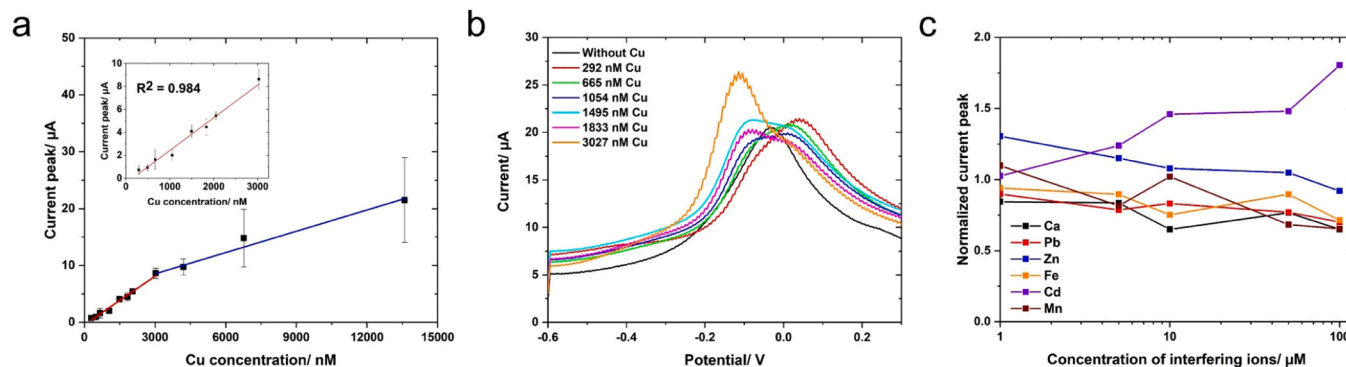

Fig. 4. Calibration curve of the bare electrode without microchannel for Cu using SWASV(a). (b) Current peak of Cu using SWASV. (c) Interference studies of Cu current peak in 10 μM Cu containing 1, 5, 10, 50, 100 μM Ca, Fe, Cd, Mn, Pb and Zn, respectively. Deposition time – 0.6 V, deposition time 180 s, SW amplitude 35 mV, step potential 5 mV, pulse width 5 ms.

about − 0.1 V, next to the acetate adsorption peak at 0 V [68,69] (Fig. 4b).

The verification of sensing selectivity was conducted by testing and calculating the changes of the peak current in the presence of other metal ions [34]. In this interference study, we selected Ca, Pb, Zn, Fe, Cd and Mn as the interfering ions, which were the most abundant metals in the aerosol samples [70–72]. The influence by each of these interfering ions in the concentration range of 1–100 μM were separately studied in the presence of 10 μM Cu. In general, Cd and Zn increased the current peak of Cu on average by 40.2% and 10.0% respectively, whereas Ca, Pb, Fe and Mn suppressed the Cu current peak by 25.1%, 20.3%, 16% and 14.6% respectively (Fig. 4c). The possible reason was that Cd and Zn formed an alloy with Cu [73,74] and were stripped from the gold surface simultaneously, while some of the other ions might compete with Cu to occupy electroactive sites on gold surface. The observed peak potential deviations were partly attributed to the potential drift of the pseudo Pt reference electrode.

3.4. Collection and sensing performance using the laboratory generated metal aerosol

FTIR result indicated that O-H, C-H, C-O, and S=O stretching peaks were enhanced in the 3550–3200, 3100–3000, 1210–1163, and 1070–1030 cm^{-1} regions, respectively, due to the cleaning of the inner surface of the microchannel before measurements (Fig. S6). A solution of 5 μM $Cu(NO_3)_2$ was used to generate soluble Cu aerosol with an arithmetic mean diameter of 36.9 ± 0.6 nm (Fig. 5a). For Cu aerosol, $PM_{0.5}$, $PM_{0.5-1}$, $PM_{1-2.5}$ and $PM_{2.5-10}$ accounted for 78.1%, 18.5%, 3.2%, and 0.2%, respectively (Fig. 5b). ICP-MS results indicated that the Cu concentration of liquid samples in the microchannel and the concentration on the microchannel wall accounted for 90% and 10% of total concentration in collected samples, respectively (Fig. S7), indicating no significant adsorption of Cu onto the microchannel wall. To obtain stable and high electrochemical signals, the effect of ultrasonic treatment was investigated to improve the metal dissolution from aerosol particles and its mass transport. The detection ratio varied in the range of 10–98% in the measurements without ultrasonic treatment (Fig. S8). Here, the detection ratio was the ratio of Cu concentration derived from electrochemical signals based on the calibration curve of the bare electrode to the ICP-MS verified concentration. In contrast, ultrasonic treatment resulted in a stabilized but lower detection ratio in the range of 10–20%. Distribution of collected particles, liquid movement, metal dissolution and distribution in the microchannel were involved and possibly resulted in low detection ratio. Therefore, the low detection ratio was investigated using malachite green particles with an arithmetic mean diameter of 79 nm (Fig. S9a). Despite the lower number of larger particles, the color was much darker around the inlet where large particles with larger mass are collected (Fig. S9b). The dissolved malachite green particles were not sufficiently distributed in solution after introduction of the liquid (Fig. S9c). With a typical diffusion-layer thickness around 40–50 μm [75], the concentration of target metal could be highly heterogeneous in local areas around the electrode, which caused the unstable detection ratio in the range of 10–98%. In comparison, the distribution equilibrium with less distinguishable concentration gradient was achieved after ultrasonic treatment (Fig. S9d). Therefore, the more uniform distribution of Cu ions in the microchannel was likely to give the low detection ratio by stabilizing the local concentration around the electrode.

The inter-chip reproducibility of the proposed microsystem was further investigated by testing Cu aerosol in the aqueous concentration range of 2–8 μM, which is the ratio of total Cu mass to the volume of the microchannel. For each microsystem, the sensing performance corresponding to the concentration of Cu is linear ($R^2 > 0.83$) (Fig. S10a). Cu concentrations derived from electrochemical signals account for 14 ± 4% of the ICPMS-verified concentrations in the microchannel (Fig. S10b), indicating the equilibrium of concentration gradient after

2 min ultrasonic treatment. The linear relationship ($R^2 = 0.86$) between ICPMS-verified concentration and current peak is again confirmed by four microsystems (Fig. 5c), which supports the reproducibility of the microsystem. According to the global regression, the limit of detection is 1.5 μM, and the total amount of Cu in the microchannel is 21 ng, which means the microsystem is able to detect the accumulated aerosol particles with soluble Cu above 21 ng. Previous study demonstrates that copper in the particulate matter exists in the divalent state, such as hydrated copper sulfate [76], so the sensing performance of the microsystem is less likely to be affected by Cu(I). According to the collection efficiency of NaCl particles, the collection efficiency of 70% is assumed at the working flow rate of 3.1 L/min, therefore, the microsystem is able to detect aerosol samples with a soluble Cu concentration higher than 32 ng/m^3 based on 5 h aerosol collection period, while the limit of detection could be further reduced to 8 ng/m^3 for a collection time of 20 h. This microsystem is applicable in a relatively short collection time at the working flow rate of 3.1 L/min with the reported Cu concentrations, such as 24.4, 117 ± 163.3, and 188 ng/m^3 in Switzerland [71], China [72], and São Paulo, Brazil [77], respectively.

3.5. Sensing performance of the microsystem using real-world samples

The arithmetic mean diameter of the PM_{10}-like aerosol was 57.1 ± 0.6 nm (Fig. 5d). In comparison to Cu aerosol, the PM_{10}-like aerosol contained a larger fraction of coarse particles to simulate the real-world environment (Fig. 5b). In particulate, $PM_{0.5}$, $PM_{0.5-1}$, $PM_{1-2.5}$ and $PM_{2.5-10}$ account for 52.7%, 42.1%, 5.0%, and 0.2% in terms of particle number, respectively. In fact, the number size distribution of the PM_{10}-like aerosol was quite similar to that of the real-world environment with a mode diameter smaller than 100 nm such as central Los Angeles [61] and London [78]. Based on the calibration curve of a single microsystem (Microsystem 4), the average detection ratio of Cu in the PM_{10}-like aerosol was 100 ± 14% (Fig. 5e), which suggests that the simultaneous presence of multiple elements such as Cd, Mn, Zn and organic matters has a minor effect on the sensing performance. It also indicates that metallic copper or the insoluble fraction of particulate copper has a limited effect on the detection of soluble copper ions. In this part, it should be noted that the detection ratio is the ratio of Cu concentration derived from electrochemical signals based on the calibration curve of the microsystem to the ICPMS-verified concentration. Collection and dissolution of the PM_{10}-liked aerosol also suggest the considerable quantity of black carbon distributes around the inlet and first turn of the microchannel, which prevents significant fouling of the electrode surface (Fig. S11). In addition, collected particles are removed by ultrasonic treatment each time after collection and detection, which prevents particle accumulation especially the insoluble fraction, and worse collection and detection performance. Unlike the sharp current peak of Cu solution, the wider and flat current peak of PM_{10}-like aerosol indicated that the oxidation peak of Cu at − 0.2 V tends to overlap with the acetate adsorption peak at a more positive potential (i.e. 0 V) (Fig. 5f). This evidence suggests that deposited Cu on the electrode surface tends to be stripped at a more positive potential when a higher concentration of PM_{10}-like aerosol samples is present in the microchannel. The possible reason is that multiple anions in the PM_{10}-like aerosol, such as sulfate [79], chloride [80] and bromide [81], affect the deposition of Cu on the gold electrode by changing the surface structures and onset potentials of the deposition process, which further influences the corresponding stripping process of Cu. Unlike the interference studies of several metal ions shown in Fig. 4c, multiple elements present in the real-world aerosol mainly affected the shape of the current peak rather than the current peak intensity (Fig. 5e and f). Therefore, the results indicated that the microsystem can be applied for practical usage despite interferences from other components such as non-target metal ions. Overall, the collection and sensing performance of the microsystem was validated by real-world aerosol containing metals, carbons, non-metal fractions. Besides that, the performance of this microsystem should be
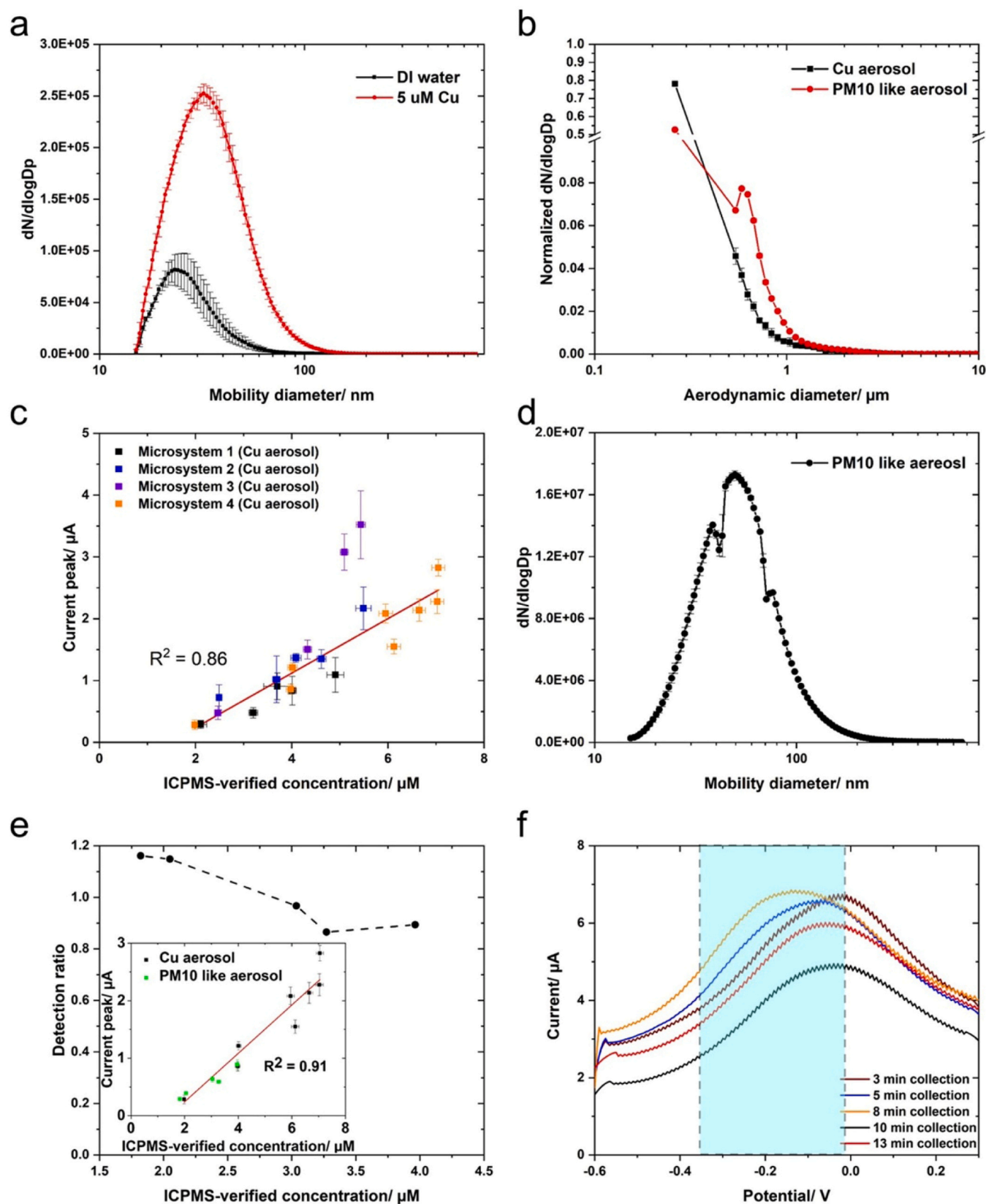
Fig. 5. Collection and electrochemical detection of aerosol metals using the microsystem: (a) SMPS results of the particle size distribution and particle numbers of the Cu aerosol; (b) Normalized particle size distribution of the Cu aerosol and PM_{10} like aerosol in terms of aerodynamic diameter; (c) Responses of electrochemical signal to lab-generated Cu aerosol using four microsystems in terms of the collection duration; (d) SMPS results of the particle size distribution and particle numbers of the PM_{10} like aerosol; (e) Detection ratio of the electrochemical signals of Cu in the PM_{10} like samples to ICP-MS measurement results; (f) SWV responses to Cu in the PM_{10} like aerosol.

examined in the real-world environment in the next step.

4. Conclusions

In this study, a promising integrated aerodynamic/electrochemical microsystem has been successfully developed to collect aerosol with relatively high efficiency to detect soluble copper at the nanogram level. The collection, dissolution and detection of aerosol copper rely on the air/solid and liquid/solid interface of the microchannel and do not require a bulky setup. This microsystem is a promising low-cost alternative to the cumbersome coupling in series for aerosol collection and detection platform. Nonetheless, the collection and sensing performance of this microsystem should be extensively examined in the real-world environment in future studies. The limitation of this microsystem is that the collection time could vary according to different soluble Cu concentration in different regions and cities.

The collection and determination of several metals such as Cu, Cd, Pb, Fe and Ni can be achieved on the current or modified microsystem (by replacing or modifying the electrode). Besides that, bioaccessiblity of aerosol metals could be extensively explored by using different leaching agents such as water, salt solutions, buffer solutions and synthetic body fluids [5], and detected in situ by the microsystem. In this way, high-resolution monitoring and investigation of bioaccessible aerosol metals could give the rapid response to air quality in terms of human health and facilitate the development of air quality control policies [8]. Furthermore, the application of the microsystem is reasonably extended to the collection and detection of other soluble elements such as nitrate [82] and aerosol oxidative load [83], which offers a new way to develop the online, mobile, low-cost and miniaturized monitoring system for different aerosol components. Therefore, a more comprehensive routine monitoring network of aerosol soluble metals and other components is potentially established to investigate the aerosol processes and protect the human health.

Author Contributions

Y.-B. Zhao and **J. Wang** conceived of the idea and designed the study. **Y.-B. Zhao** conducted the experiments, data analysis, and manuscript preparation. **J. Wang** and **C. Ludwig** contributed to the revision of the manuscript. **J. Tang** prepared the microfluidic chips. **T. Cen** and **C. Ludwig** conducted the ICP-MS measurements. **G. Qiu, W. He, F. Jiang** and **R. Yu** helped with the sensing experiments and data analysis. All authors have discussed the results and approved the final version of the manuscript.

Notes

The authors declare no competing financial interest.

CRediT authorship contribution statement

Yi-Bo Zhao: Conceptualization, Methodology, Investigation, Writing – original draft. **Jiukai Tang:** Investigation, Resources, Formal analysis. **Tianyu Cen:** Investigation, Validation, Formal analysis. **Guangyu Qiu:** Formal analysis, Data curation. **Weidong He:** Formal analysis. **Fuze Jiang:** Resources, Data curation. **Ranxue Yu:** Formal analysis. **Christian Ludwig:** Validation, Formal analysis, Writing – review & editing. **Jing Wang:** Conceptualization, Resources, Writing – review & editing, Supervision.

Declaration of Competing Interest

The authors declare that they have no known competing financial interests or personal relationships that could have appeared to influence the work reported in this paper.

Appendix A. Supplementary material

Supplementary data associated with this article can be found in the online version at doi:10.1016/j.snb.2021.130903.

References

[1] K.R. Daellenbach, G. Uzu, J. Jiang, L.-E. Cassagnes, Z. Leni, A. Vlachou, G. Stefenelli, F. Canonaco, S. Weber, A. Segers, J.J.P. Kuenen, M. Schaap, O. Favez, A. Albinet, S. Aksoyoglu, J. Dommen, U. Baltensperger, M. Geiser, I. El Haddad, J.-L. Jaffrezo, A.S.H. Prévôt, Sources of particulate-matter air pollution and its oxidative potential in Europe, Nature 587 (2020) 414–419.
[2] N.M. Mahowald, D.S. Hamilton, K.R.M. Mackey, J.K. Moore, A.R. Baker, R. A. Scanza, Y. Zhang, Aerosol trace metal leaching and impacts on marine microorganisms, Nat. Commun. 9 (2018) 2614.
[3] H. Li, X. Qian, Qg Wang, Heavy metals in atmospheric particulate matter: a comprehensive understanding is needed for monitoring and risk mitigation, Environ. Sci. Technol. 47 (2013) 13210–13211.
[4] G. Pérez, M. López-Mesas, M. Valiente, Assessment of heavy metals remobilization by fractionation: comparison of leaching tests applied to roadside sediments, Environ. Sci. Technol. 42 (2008) 2309–2315.
[5] A. Mukhtar, A. Limbeck, Recent developments in assessment of bio-accessible trace metal fractions in airborne particulate matter: a review, Anal. Chim. Acta 774 (2013) 11–25.
[6] X. Hu, Y. Zhang, Z. Ding, T. Wang, H. Lian, Y. Sun, J. Wu, Bioaccessibility and health risk of arsenic and heavy metals (Cd, Co, Cr, Cu, Ni, Pb, Zn and Mn) in TSP and PM2.5 in Nanjing, China, Atmos. Environ. 57 (2012) 146–152.
[7] T. Fang, H. Guo, L. Zeng, V. Verma, A. Nenes, R.J. Weber, Highly acidic ambient particles, soluble metals, and oxidative potential: a link between sulfate and aerosol toxicity, Environ. Sci. Technol. 51 (2017) 2611–2620.
[8] B. Zhao, L. Yu, C. Wang, C. Shuai, J. Zhu, S. Qu, M. Taiebat, M. Xu, Urban air pollution mapping using fleet vehicles as mobile monitors and machine learning, Environ. Sci. Technol. 55 (2021) 5579–5588.
[9] D. Wang, M.M. Shafer, J.J. Schauer, C. Sioutas, A new technique for online measurement of total and water-soluble copper (Cu) in coarse particulate matter (PM), Environ. Pollut. 199 (2015) 227–234.
[10] D. Wang, P. Pakbin, A. Saffari, M.M. Shafer, J.J. Schauer, C. Sioutas, Development and evaluation of a high-volume aerosol-into-liquid collector for fine and ultrafine particulate matter, Aerosol Sci. Technol. 47 (2013) 1226–1238.
[11] D. Wang, M.M. Shafer, J.J. Schauer, C. Sioutas, Development of a technology for online measurement of total and water-soluble copper (Cu) in PM2.5, Aerosol Sci. Technol. 48 (2014) 864–874.
[12] D.A. Orsini, Y. Ma, A. Sullivan, B. Sierau, K. Baumann, R.J. Weber, Refinements to the particle-into-liquid sampler (PILS) for ground and airborne measurements of water soluble aerosol composition, Atmos. Environ. 37 (2003) 1243–1259.
[13] H.R. Kim, S. An, J. Hwang, Aerosol-to-hydrosol sampling and simultaneous enrichment of airborne bacteria for rapid biosensing, ACS Sens. 5 (2020) 2763–2771.
[14] J. Bhardwaj, M.-W. Kim, J. Jang, Rapid airborne influenza virus quantification using an antibody-based electrochemical paper sensor and electrostatic particle concentrator, Environ. Sci. Technol. 54 (2020) 10700–10712.
[15] I.V. Novosselov, R.A. Gorder, J.A. Van Amberg, P.C. Ariessohn, Design and performance of a low-cost micro-channel aerosol collector, Aerosol Sci. Technol. 48 (2014) 822–830.
[16] Y. Xie, J. Rufo, R. Zhong, J. Rich, P. Li, K.W. Leong, T.J. Huang, Microfluidic isolation and enrichment of nanoparticles, ACS Nano 14 (2020) 16220–16240.
[17] X. Bian, Y. Lan, B. Wang, Y.S. Zhang, B. Liu, P. Yang, W. Zhang, L. Qiao, Microfluidic air sampler for highly efficient bacterial aerosol collection and identification, Anal. Chem. 88 (2016) 11504–11512.
[18] J. Choi, S.C. Hong, W. Kim, J.H. Jung, Highly enriched, controllable, continuous aerosol sampling using inertial microfluidics and its application to real-time detection of airborne bacteria, ACS Sens. 2 (2017) 513–521.
[19] W. Jing, W. Zhao, S. Liu, L. Li, C.-T. Tsai, X. Fan, W. Wu, J. Li, X. Yang, G. Sui, Microfluidic device for efficient airborne bacteria capture and enrichment, Anal. Chem. 85 (2013) 5255–5262.
[20] S.C. Hong, J.S. Kang, J.E. Lee, S.S. Kim, J.H. Jung, Continuous aerosol size separator using inertial microfluidics and its application to airborne bacteria and viruses, Lab Chip 15 (2015) 1889–1897.
[21] I. Mirzaee, M. Song, M. Charmchi, H. Sun, A microfluidics-based on-chip impinger for airborne particle collection, Lab Chip 16 (2016) 2254–2264.

[22] W. Zhang, H. Zhang, S.E. Williams, A. Zhou, Microfabricated three-electrode on-chip PDMS device with a vibration motor for stripping voltammetric detection of heavy metal ions, Talanta 132 (2015) 321–326.

[23] J. Wang, P. Yu, K. Kan, H. Lv, Z. Liu, B. Sun, J. Bai, J. Chen, Y. Zhang, K. Shi, Efficient ultra-trace electrochemical detection of Cd^{2+}, Pb^{2+} and Hg^{2+} based on hierarchical porous S-doped C_3N_4 tube bundles/graphene nanosheets composite, Chem. Eng. J. 420 (2021), 130317.

[24] N. Ullah, M. Mansha, I. Khan, A. Qurashi, Nanomaterial-based optical chemical sensors for the detection of heavy metals in water: recent advances and challenges, TrAC Trend Anal. Chem. 100 (2018) 155–166.

[25] C.-Y. Wang, C.-C. Hsu, Online, continuous, and interference-free monitoring of trace heavy metals in water using plasma spectroscopy driven by actively modulated pulsed power, Environ. Sci. Technol. 53 (2019) 10888–10896.

[26] G. Qiu, S.P. Ng, X. Liang, N. Ding, X. Chen, C.-M.L. Wu, Label-free LSPR detection of trace lead(II) ions in drinking water by synthetic poly(mPD-co-ASA) nanoparticles on gold nanoislands, Anal. Chem. 89 (2017) 1985–1993.

[27] D. Wang, M.H. Sowlat, M.M. Shafer, J.J. Schauer, C. Sioutas, Development and evaluation of a novel monitor for online measurement of iron, manganese, and chromium in ambient particulate matter (PM), Sci. Total Environ. 565 (2016) 123–131.

[28] G. Aragay, J. Pons, A. Merkoçi, Recent trends in macro-, micro-, and nanomaterial-based tools and strategies for heavy-metal detection, Chem. Rev. 111 (2011) 3433–3458.

[29] J. Kudr, O. Zitka, M. Klimanek, R. Vrba, V. Adam, Microfluidic electrochemical devices for pollution analysis – a review, Sens. Actuators B: Chem. 246 (2017) 578–590.

[30] D. Buzica, M. Gerboles, A. Borowiak, P. Trincherini, R. Passarella, V. Pedroni, Comparison of voltammetry and inductively coupled plasma-mass spectrometry for the determination of heavy metals in PM10 airborne particulate matter, Atmos. Environ. 40 (2006) 4703–4710.

[31] S. Li, C. Zhang, S. Wang, Q. Liu, H. Feng, X. Ma, J. Guo, Electrochemical microfluidics techniques for heavy metal ion detection, Analyst 143 (2018) 4230–4246.

[32] K. Pi, J. Liu, P. Van Cappellen, Direct measurement of aqueous mercury(II): combining DNA-based sensing with diffusive gradients in thin films, Environ. Sci. Technol. 54 (2020) 13680–13689.

[33] D. Neagu, F. Arduini, J.C. Quintana, P. Di Cori, C. Forni, D. Moscone, Disposable electrochemical sensor to evaluate the phytoremediation of the aquatic plant Lemna minor L. toward Pb^{2+} and/or Cd^{2+}, Environ. Sci. Technol. 48 (2014) 7477–7485.

[34] J. Mettakoonpitak, J. Volckens, C.S. Henry, Janus electrochemical paper-based analytical devices for metals detection in aerosol samples, Anal. Chem. 92 (2020) 1439–1446.

[35] A. Fernández-la-Villa, D.F. Pozo-Ayuso, M. Castaño-Álvarez, Microfluidics and electrochemistry: an emerging tandem for next-generation analytical microsystems, Curr. Opin. Electrochem. 15 (2019) 175–185.

[36] R. Wang, X. Wang, Sensing of inorganic ions in microfluidic devices, Sens. Actuators B: Chem. 329 (2021), 129171.

[37] A. Chałupniak, A. Merkoçi, Graphene oxide–poly(dimethylsiloxane)-based lab-on-a-chip platform for heavy-metals preconcentration and electrochemical detection, ACS Appl. Mater. Interfaces 9 (2017) 44766–44775.

[38] A. Jang, Z. Zou, K.K. Lee, C.H. Ahn, P.L. Bishop, Potentiometric and voltammetric polymer lab chip sensors for determination of nitrate, pH and Cd(II) in water, Talanta 83 (2010) 1–8.

[39] P.N. Nge, C.I. Rogers, A.T. Woolley, Advances in microfluidic materials, functions, integration, and applications, Chem. Rev. 113 (2013) 2550–2583.

[40] A.R. Metcalf, S. Narayan, C.S. Dutcher, A review of microfluidic concepts and applications for atmospheric aerosol science, Aerosol Sci. Technol. 52 (2018) 310–329.

[41] Y. Sameenoi, K. Koehler, J. Shapiro, K. Boonsong, Y. Sun, J. Collett, J. Volckens, C.S. Henry, Microfluidic electrochemical sensor for on-line monitoring of aerosol oxidative activity, J. Am. Chem. Soc. 134 (2012) 10562–10568.

[42] S.D. Noblitt, G.S. Lewis, Y. Liu, S.V. Hering, J.L. Collett, C.S. Henry, Interfacing microchip electrophoresis to a growth tube particle collector for semicontinuous monitoring of aerosol composition, Anal. Chem. 81 (2009) 10029–10037.

[43] J. Mettakoonpitak, D. Miller-Lionberg, T. Reilly, J. Volckens, C.S. Henry, Low-cost reusable sensor for cobalt and nickel detection in aerosols using adsorptive cathodic square-wave stripping voltammetry, J. Electroanal. Chem. 805 (2017) 75–82.

[44] J. Mettakoonpitak, J. Mehaffy, J. Volckens, C.S. Henry, AgNP/Bi/nafion-modified disposable electrodes for sensitive Zn(II), Cd(II), and Pb(II) detection in aerosol samples, Electroanalysis 29 (2017) 880–889.

[45] M.R. Palomo-Marín, F. Rueda-Holgado, J. Marín-Expósito, E. Pinilla-Gil, Disposable sputtered-bismuth screen-printed sensors for voltammetric monitoring of cadmium and lead in atmospheric particulate matter samples, Talanta 175 (2017) 313–317.

[46] F. Rueda-Holgado, E. Bernalte, M.R. Palomo-Marín, L. Calvo-Blázquez, F. Cereceda-Balic, E. Pinilla-Gil, Miniaturized voltammetric stripping on screen printed gold electrodes for field determination of copper in atmospheric deposition, Talanta 101 (2012) 435–439.

[47] F. Rueda-Holgado, L. Calvo-Blázquez, F. Cereceda-Balic, E. Pinilla-Gil, A semiautomatic system for soluble lead and copper monitoring in atmospheric deposition by coupling of passive elemental fractionation sampling and voltammetric measurement on screen-printed gold electrodes, Microchem. J. 124 (2016) 20–25.

[48] S. Canepari, M.L. Astolfi, S. Moretti, R. Curini, Comparison of extracting solutions for elemental fractionation in airborne particulate matter, Talanta 82 (2010) 834–844.

[49] K.J. Regehr, M. Domenech, J.T. Koepsel, K.C. Carver, S.J. Ellison-Zelski, W.L. Murphy, L.A. Schuler, E.T. Alarid, D.J. Beebe, Biological implications of polydimethylsiloxane-based microfluidic cell culture, Lab Chip 9 (2009) 2132–2139.

[50] A. Hourlier-Fargette, J. Dervaux, A. Antkowiak, S. Neukirch, Extraction of silicone uncrosslinked chains at air–water–polydimethylsiloxane triple lines, Langmuir 34 (2018) 12244–12250.

[51] C. Provin, T. Fujii, Reaction–diffusion phenomena in a PDMS matrix can modify its topography, Lab Chip 11 (2011) 2948–2954.

[52] Z. Almutairi, C.L. Ren, L. Simon, Evaluation of polydimethylsiloxane (PDMS) surface modification approaches for microfluidic applications, Colloids Surf. A 415 (2012) 406–412.

[53] X. Sun, R.T. Kelly, K. Tang, R.D. Smith, Ultrasensitive nanoelectrospray ionization-mass spectrometry using poly(dimethylsiloxane) microchips with monolithically integrated emitters, Analyst 135 (2010) 2296–2302.

[54] J. Lee, N. Jäckel, D. Kim, M. Widmaier, S. Sathyamoorthi, P. Srimuk, C. Kim, S. Fleischmann, M. Zeiger, V. Presser, Porous carbon as a quasi-reference electrode in aqueous electrolytes, Electrochim. Acta 222 (2016) 1800–1805.

[55] Y. Lu, X. Liang, C. Niyungeko, J. Zhou, J. Xu, G. Tian, A review of the identification and detection of heavy metal ions in the environment by voltammetry, Talanta 178 (2018) 324–338.

[56] L. Gitlin, P. Schulze, S. Ohla, H.-J. Bongard, D. Belder, Surface modification of PDMS microfluidic devices by controlled sulfuric acid treatment and the application in chip electrophoresis, Electrophoresis 36 (2015) 449–456.

[57] Z. Zou, A. Jang, E. MacKnight, P.-M. Wu, J. Do, P.L. Bishop, C.H. Ahn, Environmentally friendly disposable sensors with microfabricated on-chip planar bismuth electrode for in situ heavy metal ions measurement, Sens. Actuators B: Chem. 134 (2008) 18–24.

[58] G. Emma, J. Snell, J. Charoud-Got, A. Held, H. Emons, Feasibility study of a candidate reference material for ions in PM2.5: does commutability matter also for inorganic matrices? Anal. Bioanal. Chem. 410 (2018) 6001–6008.

[59] K. Ashley, R.N. Andrews, L. Cavazos, M. Demange, Ultrasonic extraction as a sample preparation technique for elemental analysis by atomic spectrometry, J. Anal. At. Spectrom. 16 (2001) 1147–1153.

[60] European Commission's Joint Research Centre, CERTIFICATE OF ANALYSIS ERM®-CZ120, 2010. ⟨https://crm.jrc.ec.europa.eu/p/40454/40470/By-applica tion-field/Environment/ERM-CZ120-FINE-DUST-PM10-LIKE-elements/ER M-CZ120⟩.

[61] S. Taghvaee, A. Mousavi, M.H. Sowlat, C. Sioutas, Development of a novel aerosol generation system for conducting inhalation exposures to ambient particulate matter (PM), Sci. Total Environ. 665 (2019) 1035–1045.

[62] L. Baldrianova, P. Agrafiotou, I. Svancara, A.D. Jannakoudakis, S. Sotiropoulos, The effect of acetate concentration, solution pH and conductivity on the anodic stripping voltammetry of lead and cadmium ions at in situ bismuth-plated carbon microelectrodes, J. Electroanal. Chem. 660 (2011) 31–36.

[63] C.L. Reddington, G. McMeeking, G.W. Mann, H. Coe, M.G. Frontoso, D. Liu, M. Flynn, D.V. Spracklen, K.S. Carslaw, The mass and number size distributions of black carbon aerosol over Europe, Atmos. Chem. Phys. 13 (2013) 4917–4939.

[64] H. Maring, D.L. Savoie, M.A. Izaguirre, L. Custals, J.S. Reid, Mineral dust aerosol size distribution change during atmospheric transport, J. Geophys. Res.: Atmos. 108 (2003) 8592.

[65] X. Pei, W. Kang, W. Yue, A. Bange, W.R. Heineman, I. Papautsky, Disposable copper-based electrochemical sensor for anodic stripping voltammetry, Anal. Chem. 86 (2014) 4893–4900.

[66] W. Kang, X. Pei, C.A. Rusinek, A. Bange, E.N. Haynes, W.R. Heineman, I. Papautsky, Determination of lead with a copper-based electrochemical sensor, Anal. Chem. 89 (2017) 3345–3352.

[67] J. Holmes, P. Pathirathna, P. Hashemi, Novel frontiers in voltammetric trace metal analysis: towards real time, on-site, in situ measurements, TrAC Trends Anal. Chem. 111 (2019) 206–219.

[68] C.P. Byers, B.S. Hoener, W.-S. Chang, S. Link, C.F. Landes, Single-particle plasmon voltammetry (spPV) for detecting anion adsorption, Nano Lett. 16 (2016) 2314–2321.

[69] A. Berná, J.M. Delgado, J.M. Orts, A. Rodes, J.M. Feliu, Spectroelectrochemical study of the adsorption of acetate anions at gold single crystal and thin-film electrodes, Electrochim. Acta 53 (2008) 2309–2321.

[70] Y. Yue, H. Chen, A. Setyan, M. Elser, M. Dietrich, J. Li, T. Zhang, X. Zhang, Y. Zheng, J. Wang, M. Yao, Size-resolved endotoxin and oxidative potential of ambient particles in Beijing and Zürich, Environ. Sci. Technol. 52 (2018) 6816–6824.

[71] M. Furger, M.C. Minguillón, V. Yadav, J.G. Slowik, C. Hüglin, R. Fröhlich, K. Petterson, U. Baltensperger, A.S.H. Prévôt, Elemental composition of ambient aerosols measured with high temporal resolution using an online XRF spectrometer, Atmos. Meas. Technol. 10 (2017) 2061–2076.

[72] J. Duan, J. Tan, Atmospheric heavy metals and Arsenic in China: situation, sources and control policies, Atmos. Environ. 74 (2013) 93–101.

[73] N.T. Tuan, J. Park, J. Lee, J. Gwak, D. Lee, Synthesis of nanoporous Cu films by dealloying of electrochemically deposited Cu–Zn alloy films, Corros. Sci. 80 (2014) 7–11.

[74] B. Bozzini, P.L. Cavallotti, Electrodeposition and characterization of Au–Cu–Cd alloys, J. Appl. Electrochem 31 (2001) 897–903.

[75] J.Y. Gao, Studying dissolution with a model integrating solid–liquid interface kinetics and diffusion kinetics, Anal. Chem. 84 (2012) 10671–10678.

[76] F.E. Huggins, G.P. Huffman, J.D. Robertson, Speciation of elements in NIST particulate matter SRMs 1648 and 1650, J. Hazard. Mater. 74 (2000) 1–23.

[77] G.M. Pereira, K. Teinilä, D. Custódio, A. Gomes Santos, H. Xian, R. Hillamo, C. A. Alves, J. Bittencourt de Andrade, G. Olímpio da Rocha, P. Kumar, R. Balasubramanian, M.D.F. Andrade, P. de Castro Vasconcellos, Particulate pollutants in the Brazilian city of São Paulo: 1-year investigation for the chemical composition and source apportionment, Atmos. Chem. Phys. 17 (2017) 11943–11969.

[78] R.M. Harrison, D.C.S. Beddows, M.S. Alam, A. Singh, J. Brean, R. Xu, S. Kotthaus, S. Grimmond, Interpretation of particle number size distributions measured across an urban area during the FASTER campaign, Atmos. Chem. Phys. 19 (2019) 39–55.

[79] B. Madry, K. Wandelt, M. Nowicki, Sulfate structures on copper deposits on Au (111): in situ STM investigations, Electrochim. Acta 217 (2016) 249–261.

[80] F. Möller, O.M. Magnussen, R.J. Behm, CuCl adlayer formation and Cl induced surface alloying: an in situ STM study on Cu underpotential deposition on Au(110) electrode surfaces, Electrochim. Acta 40 (1995) 1259–1265.

[81] E. Herrero, S. Glazier, L.J. Buller, H.D. Abruña, X-ray and electrochemical studies of Cu upd on single crystal electrodes in the presence of bromide: comparison between Au(111) and Pt(111) electrodes, J. Electroanal. Chem. 461 (1999) 121–130.

[82] L. Yu, Q. Zhang, Q. Xu, D. Jin, G. Jin, K. Li, X. Hu, Electrochemical detection of nitrate in PM2.5 with a copper-modified carbon fiber micro-disk electrode, Talanta 143 (2015) 245–253.

[83] K.A. Koehler, J. Shapiro, Y. Sameenoi, C. Henry, J. Volckens, Laboratory evaluation of a microfluidic electrochemical sensor for aerosol oxidative load, Aerosol Sci. Technol. 48 (2014) 489–497.

[84] H.d.A. Silva-Neto, T.M.G. Cardoso, W.K.T. Coltro, R.C. Urban, Determination of bioavailable lead in atmospheric aerosols using unmodified screen-printed carbon electrodes, Anal. Methods 11 (2019) 4875–4881.

Yi-Bo Zhao received his M.S. degree in Natural Science from Peking University, China in 2018. He is currently pursuing his Ph.D. degree under the direction of Prof. Jing Wang at the Institute of Environmental Engineering, ETH Zürich. His research interests include aerosol sampling, aerosol trace metal determination, electrochemical sensors, and development of integrated aerodynamic/electrochemical sensing system.

Jiukai Tang is currently a Ph.D. candidate under the direction of Prof. Jing Wang at the Institute of Environmental Engineering, ETH Zürich. His research interests include optofluidics, analytical chemistry, and biosensors.

Tianyu Cen is currently a Ph.D. candidate at École polytechnique fédérale de Lausanne (EPFL). His research interests include single particle-ICP-MS and online analysis of nanoparticles in the liquid and gas phase.

Guangyu Qiu is a postdoctoral Researcher at ETH Zurich. He obtained his Ph.D. from City University of Hong Kong. His research area includes applied optics and plasmonics, functional materials in nano-optics, chemical, biochemical and environmental sensing applications.

Weidong He is pursuing her Ph.D. degree at Northeastern University, China. His research interests include air filtration and smart air filters.

Fuze Jiang is now pursuing his Ph.D. degree at the Institute of Environmental Engineering, ETH Zürich. His research interests include electrochemical biosensors, gas electrocatalysis, and development of compact electrochemical workstation.

Ranxue Yu is currently pursuing her Ph.D. degree at Donghua University, China. Her research focuses on the detection of airborne organic carbon and development of metal-coated nanofibers.

Christian Ludwig is an adjunct Professor at École polytechnique fédérale de Lausanne (EPFL) in the field of Solid Waste Treatment and head of the Chemical Processes and Materials research group (CPM) at Paul Scherrer Institute (PSI) since 2005. His recent works include nucleation and crystallization processes, size-resolved elemental analysis of gasborne nanoparticles, sorption processes for the cleaning of gases and fluids, recovery of rare earth elements and phosphor from wastes and residues, and algal biomass and its applications for waste water treatment, biofuels and chemicals.

Jing Wang is an associate professor at the Institute of Environmental Engineering in the Department of Civil, Environmental and Geomatics Engineering, ETH Zürich. He received his Ph.D. degree in Aerospace Engineering at the University of Minnesota in 2005. He worked as a postdoctoral associate in the Particle Technology Laboratory, Mechanical Engineering at the University of Minnesota. His research interests include air pollution control, nanoparticle transport and emission reduction, instrumentation for airborne nanoparticle measurement, air and water filtration, and mechanics of multiphase flow.